Journal of Sound and Vibration (2001) **245**(3), 417–431
doi:10.1006/jsvi.2001.3589, available online at http://www.idealibrary.com on IDEAL®

ROBUSTNESS OF OPTIMAL DESIGN SOLUTIONS TO REDUCE VIBRATION TRANSMISSION IN A LIGHTWEIGHT 2-D STRUCTURE, PART III: USING BOTH GEOMETRIC REDESIGN AND THE APPLICATION OF ACTIVE VIBRATION CONTROL

D. K. ANTHONY

Institute of Sound & Vibration Research, University of Southampton, Southampton SO17 1BJ, England.
E-mail: dka@soton.ac.uk

(*Received* 12 *April* 2000, *and in final form* 19 *October* 2000)

In Parts I and II of this series of papers, geometric optimization (Anthony *et al.* 2000 *Journal of Sound and Vibration* **229**, 505–528 [1]), and the application of active vibration control (AVC) techniques with optimally placed actuators (Anthony and Elliott 2000 *Journal of Sound and Vibration* **229**, 529–548 [2]) were both used to reduce the vibration transmission of a lightweight cantilever structure. Two further strategies are reported here combining these techniques: (1) the application of AVC using optimal actuator positions placed on the geometrically optimized structures reported in Part I; and (2) the simultaneous optimization of the structure geometry and the AVC actuator positions.

For both strategies even better vibration reductions were found than in references [1, 2]. The application of AVC is seen to be more efficient (reduction per AVC control effort) if the structure geometry is also optimized. Slightly better reductions were found with the simultaneous optimization strategy. The change in the performance of the optimal structures due to small geometric perturbations, representing manufacturing tolerances for example, is investigated by a robustness analysis. It was found, as before, that the selection of the best practical structure is not necessarily the same structure ranked on nominal performance, and the AVC control effort can also increase dramatically in the face of such geometric perturbations.

Finally, a comparison of the average success of using all the optimization strategies considered in Parts I and II, and in this paper are compared for both the performance and control effort required (where applicable), for both nominal and perturbed structure geometries.

1. INTRODUCTION

This is the final companion paper concerned with the reduction of vibration transmission of a two-dimensional (2-D) lightweight structure. *Passive optimization* techniques were used in Part I, where the structure geometry was redesigned [1], and *active optimization* techniques, the application of feedforward active vibration control (AVC) to the original structure geometry, in Part II [2]. The results of two more strategies are reported: the use of AVC with optimal actuator positions on the previously geometrically optimized structures reported in reference [1], and the optimization of the structure geometry and optimized actuator positions for an AVC system simultaneously. Due to the nature of the optimization problem, when optimizing both the geometry and the actuator positions,

0022-460X/01/330417 + 15 $35.00/0

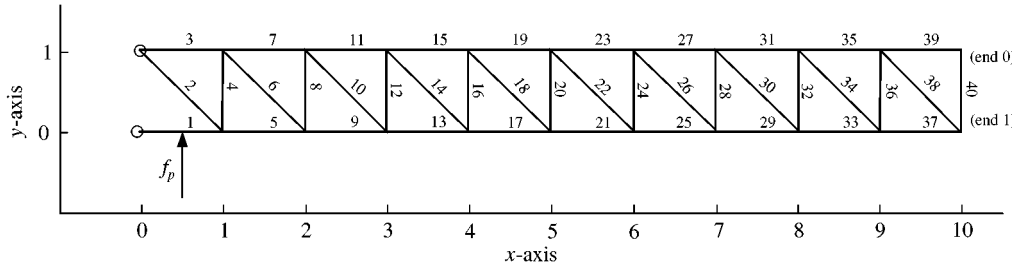

Figure 1. Unoptimized structure showing co-ordinate system, primary input force position and beam numbering scheme.

which often also involve discrete variables, so-called Natural Algorithms, such as genetic algorithms [3] or simulated annealing [4] are often used.

The optimization of both a structure and AVC actuator positions has been reported by Liu *et al.* [5, 6] and Furuya [7] (for static shape correction), using simulated annealing and genetic optimization. Dhingra and Lee [8] used a hybrid genetic algorithm/gradient-based optimization scheme on a smaller 12-beam structure, where the cross-sectional area and the actuator positions are optimized in conjunction with other system parameters. The structural optimization performed here is achieved by allowing the geometry to vary. Liu *et al.* [5, 6] maintained the geometry but allowed the cross-sectional area of each beam to be variable, and even diminish to zero, so changing the topology. The author feels that this has practical disadvantages; in the requirement for custom machining of each beam, the complexities of the union between thick and very thin beams, and the likely loss of static strength due to the removal of beams. Chen *et al.* [9] maintained the geometry of the structure and individual members and used simulated annealing to find optimal positions of both active and passive damping elements (i.e., actuators and dampers) on a truss-type boom and also a larger 150-member tetrahedral truss.

If the nominal performance of the optimized structure is sensitive to small geometric perturbations then the structure is not *robust* and may not be a practical solution. It may be better to choose a solution which has an inferior nominal performance, but whose performance is more robust. The concept of robustness was introduced in reference [1], and extended to the control effort required by an AVC system in reference [2].

The subject of the study presented here, as previously in Parts I and II [1, 2], is to minimize the average vibration transmission from the structure base to the beam 40 of the lightweight 2-D structure shown in Figure 1. The base excitation was modelled as a transverse force of arbitrary value of 1 N applied to beam 1 at 0·5 m from the base end. The performance was taken as the average value of the energy level in beam 40 over the frequency range 150–250 Hz, realized in 21 5 Hz steps. Further details of the structure, the receptance model used, and the performance measure are given in reference [1]. The application of feedforward AVC to the structure using double-acting axial-operating actuators is detailed in reference [2].

Causality constraints exist when using feedforward AVC to control broadband vibration of a structure, and are dictated by signal processing delays. Due to the dispersive nature of flexural waves this becomes more stringent at higher frequencies [10]. It is assumed here that there is sufficient *advance* in the reference signal, due to the vibration source being at a sufficient distance from the structure base, so that no such constraints exist.

2. PASSIVE-THEN-ACTIVE OPTIMIZATION STRATEGY

Ten optimal structure geometries have been generated previously by geometric optimization. These correspond to structures B_A to B_J in reference [1], which were optimized to minimize the average vibration over the frequency band 150–250 Hz. The actuator positions that result in the maximum additional vibration transmission reduction over this frequency band using AVC were then found. Thus, this optimization strategy is termed *passive-then-active*. For a given number of actuators, an exhaustive search for all possible actuator combinations was performed, as detailed in reference [2]. The only difference here is that the transfer force and mobility matrices (**C** and **Y** in reference [2]) are those corresponding to the optimized structure geometries in each case and not the original, unoptimized geometry. Since an exhaustive search is performed the best actuator combinations will be found.

AVC with one to three actuators was investigated. Average values of AVC attenuation achieved using three actuators would not be practically realizable with a realistic noise floor (which would limit the reduction at a single frequency to about 60 dB). The structure that provides the best overall average reduction in vibration transmission using AVC with a single actuator is structure PTA1_B, shown in Figure 2, which has the optimized structure

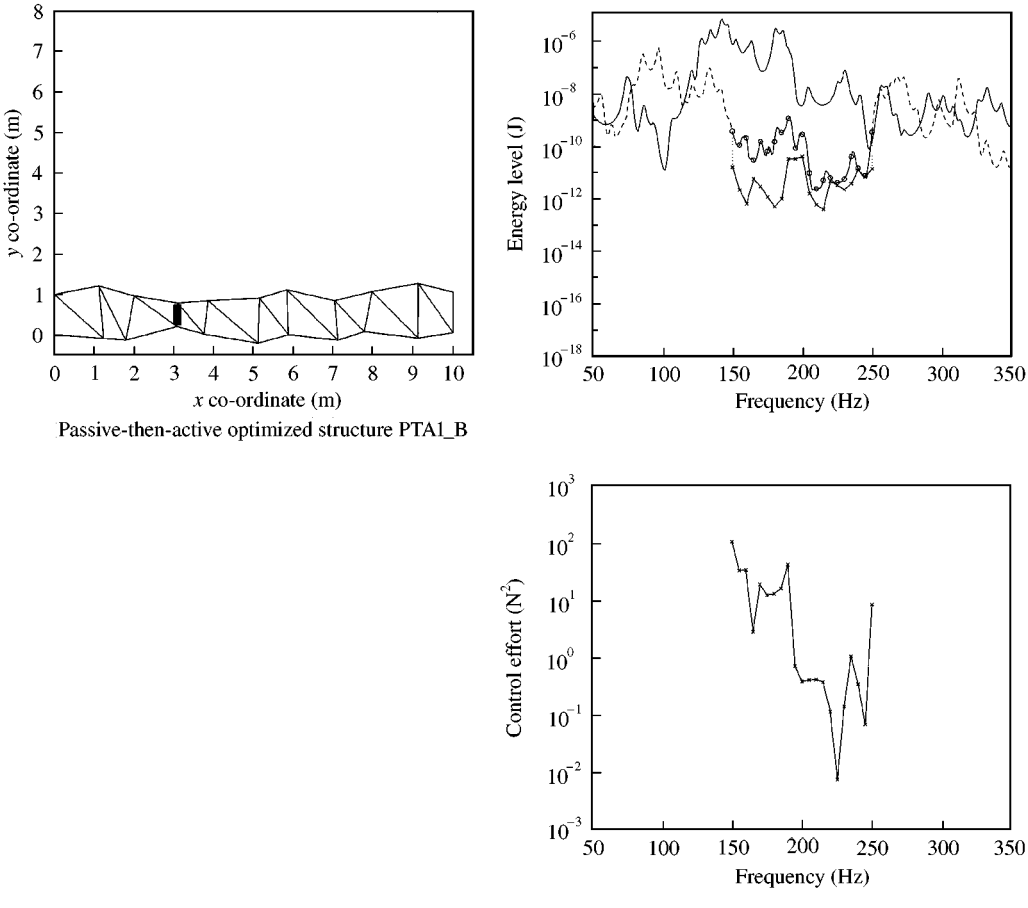

Figure 2. Best structure resulting from the passive-then-active optimization with one actuator, structure PTA1_B. (Energy level: (—) unoptimized response; (- - -) optimized response; optimization window with AVC (–×–×–); and with AVC suppressed (–○–○–).)

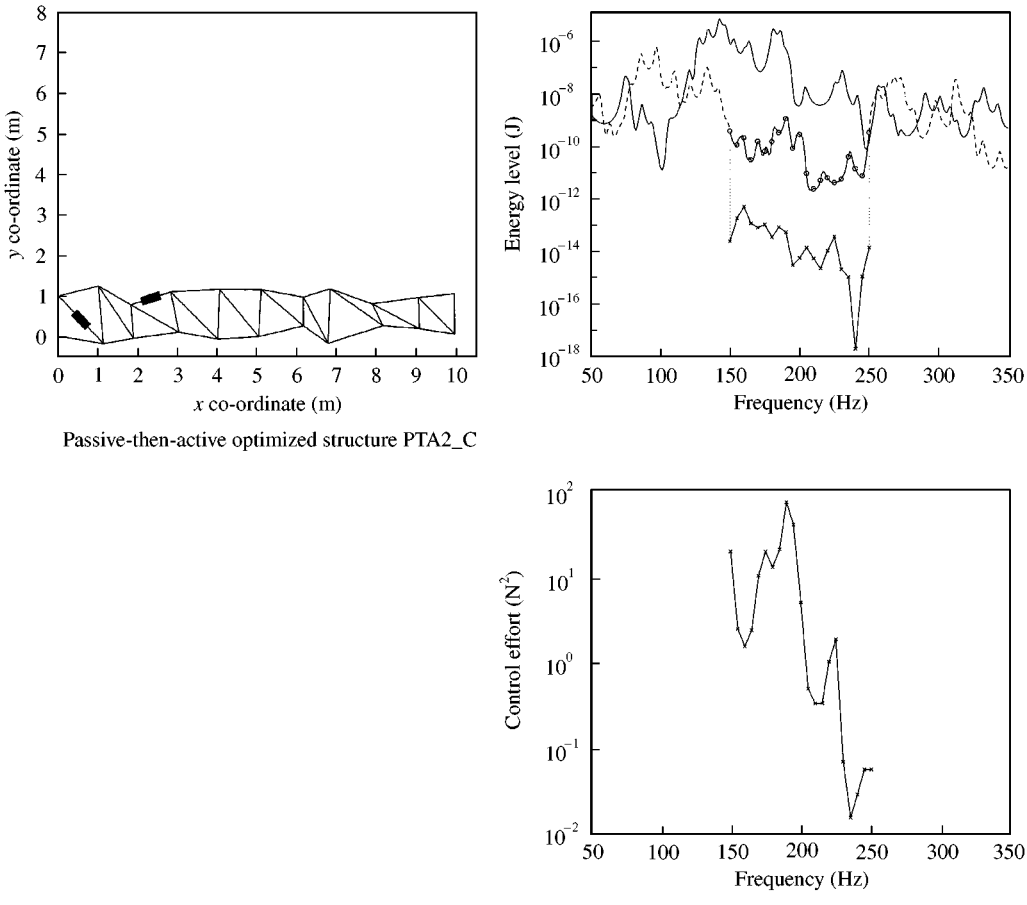

Figure 3. Best structure resulting from the passive-then-active optimization with two actuators, structure PTA2_C. (Energy level: (—) unoptimized response; (- - -) optimized response; optimization window with AVC (—×—×—); and with AVC suppressed (—○—○—).)

geometry B_B (from reference [1]). When using two optimally placed AVC actuators, the best structure is PTA2_C, as shown in Figure 3. This has the optimized structure geometry B_C [1].

It can be seen from Figures 2 and 3 that there are large variations in the additional vibration attenuation achieved at each frequency. Some of the larger values would be limited in a practical system due to noise, as mentioned above. A large variation is also seen in the control effort, spanning four orders of magnitude. (This is an indicator of electrical power required [2].)

Average values over the frequency range 150–250 Hz are presented in Tables 1 and 2 for the 10 passive-then-active structures, using one and two actuators respectively. The values of reduction are given in decibels with respect to the unoptimized structure without AVC. The two component parts of the overall vibration attenuation, that due to the geometric optimization and that due to AVC for each structure, are also given separately. The average value of attenuation for the 10 structures attributed to the AVC is similar to the values of attenuation achieved with the best actuator position(s) using AVC on the unoptimized structure geometry [2], with the same number of actuators. On average, using AVC with two actuators, the geometric and AVC reductions are of similar magnitude. Greater values

TABLE 1

Results summary for single-actuator passive-then-active optimized structures, ranked in order of performance

Rank	Structure	Geometric attenuation (dB)	AVC attenuation (dB)	Overall nominal attenuation (dB)	95% Probability limit attenuation (dB)	Control effort (N^2)	95% Probability limit control effort (N^2)
1	PTA1_B	33·3	12·7	46·0	43·0	291	467
2	PTA1_G	32·0	12·6	44·6	41·6	12·8	23·9
3	PTA1_J	32·3	12·2	44·5	41·5	22·8	30·3
4	PTA1_D	31·6	12·6	44·2	42·6	52·5	84·5
5	PTA1_H	33·9	10·1	44·0	39·6	1·52	2·46
6	PTA1_A	32·3	11·5	43·8	39·1	12·8	31·9
7	PTA1_C	32·8	10·3	43·1	38·2	345	956
8	PTA1_I	31·0	11·9	42·9	39·3	770	1850
9	PTA1_F	34·1	8·3	42·4	37·3	14·7	36·9
10	PTA1_E	34·5	5.9	40·4	38·4	24·0	46·1
Average		32·6	11·2	43·2†	39·7	155	353

TABLE 2

Results summary for two-actuator passive-then-active optimized structures, ranked in order of performance

Rank	Structure	Geometric attenuation (dB)	AVC attenuation (dB)	Overall nominal attenuation (dB)	95% Probability limit attenuation (dB)	Control effort (N^2)	95% Probability limit control effort (N^2)
1	PTA2_C	32·8	35·0	67·8	64·4	223	387
2	PTA2_A	32·3	34·7	67·0	60·2	108	387
3	PTA2_F	34·1	32·2	66·3	62·0	262	552
4	PTA2_B	33·3	32·4	65·7	62·7	25·6	32·9
5	PTA2_G	32·0	33·5	65·5	59·9	83·5	310
6	PTA2_D	31·6	31·8	63·4	58·0	79·6	119
7	PTA2_E	34·5	28·8	63·3	60·1	88·1	178
8	PTA2_H	33·9	29·0	62·9	58·3	44·5	63·7
9	PTA2_I	31·0	29·7	60·7	54·6	1060	1920
10	PTA2_J	32·3	28·3	60·6	56·7	37·3	106
Average		32·6	32·2	63·6†	58·8	201	406

†As a consequence of the logarithmic scaling, the addition of the two average components of the nominal total attenuation does not result in the average total attenuation, as with the individual cases.

of overall attenuation are achieved by applying AVC to previously optimized structure geometries due to the simple net effect of vibration reductions achieved through the geometry and the AVC. The values of control effort are also given, and a large variation of 500–50 times is seen for one and two actuators respectively. These values of control effort

are much smaller than those required when applying AVC on the unoptimized structure [2] per number of actuators used and per decibel AVC attenuation achieved. A comparison of the average control effort required with different optimization strategies is deferred until section 5.

3. COMBINED OPTIMIZATION STRATEGY

Genetic algorithms, which were used in reference [1] to optimize the structure geometry, were used to optimize the geometry and the AVC actuator positions simultaneously. This is a discrete, highly combinatorial and multimodal search space problem. However, in this case a continuous variable is used to represent the actuator positions. Apart from the extension of the chromosomes to represent the actuator positions, all the genetic algorithm parameters are identical to those used for the broadband optimization detailed in reference [1].

The Design Exploration System used, OPTIONS [11], allows a natural representation of an optimization variable as a number of discretely defined values. For one actuator, this would require a 6-bit string to represent the 39 possible beam locations. The remainder of the chromosome string represents the x and y joint co-ordinates for 18 joints, each co-ordinate being represented by a 16-bit binary string. The total chromosome length would then be 582 bits, but the actuator position representation would then be less than 1% of the chromosome's length. In order to increase the probability of the part of the chromosome representing the actuator position being affected by the crossover and mutation operations of the genetic algorithm, another method was sought in which a greater portion of the chromosome represented the positions of the actuators.

A single continuous variable (represented by a 16-bit string) was used, scaled between 0 and 1. A mapping was then used to convert the variable to actuator positions on beams 1–39, such that if a random variable with a uniform probability distribution were used to select the actuator positions, all the actuator positions would have an equal probability of selection. Similarly, for two actuators the variable was mapped on to the 741 distinct possible two-actuator combinations. Using this method the actuator positions account for 2·7% of the chromosome length, for both one and two actuators.

Ten optimized structures were produced using AVC with one and two actuators to reduce the average vibration in the frequency band 150–250 Hz. The genetic algorithm was run as 15 generations of population size 300 chromosomes. The 18 mid-structural joint co-ordinates were allowed to change by up to $\pm$ 0·25 m from their original values, as in reference [1]. The evaluation of the performance of each candidate structure to calculate the net energy level in beam 40 is detailed in reference [2]. The high-performance computational facilities used were about 3 times faster than those used for the optimizations in Part I [1], although due to the extra computation required for the AVC each optimized structure still took approximately 160 and 220 h to produce, for one and two actuators respectively.

The best structures achieved for AVC systems using one and two actuators using the combined optimization are shown in Figures 4 and 5 respectively. Also shown are the values of energy level against frequency for the unoptimized and optimized structure geometries, and the additional vibration reduction achieved by the AVC at the frequencies at which it was applied, and the AVC control effort against frequency. The value of the smallest vibration level achieved in each generation in the history of the genetic algorithm optimization is shown in the lower left-hand part, where the value relating to the original structure without AVC is shown on the y-axis using a square symbol. The initial

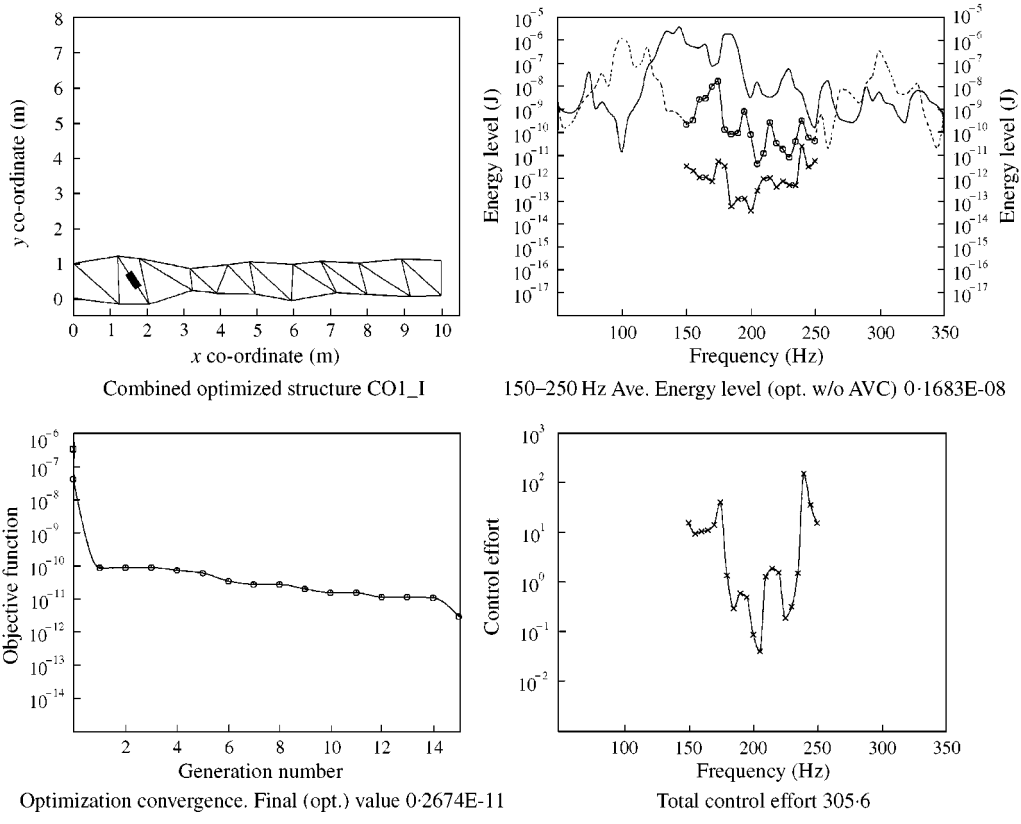

Figure 4. Best structure resulting from the combined optimization with one actuator, structure CO1_I. (Energy level: (- - - - -) unoptimized response; (– – –) optimized response; optimization window with AVC (—×—×—); and with AVC suppressed (—○—○—).)

improvement before start of the optimization is due to the application of AVC to the unoptimized structure using an arbitrary actuator position or positions.

Frequency-averaged values for all of the 10 structures produced are given in Tables 3 and 4, for one and two actuators, respectively, quoted in decibels with reference to the unoptimized structure without AVC. Again, the two constituent components of the vibration reductions, the contributions from the geometric optimization and the AVC, are shown separately. On average, it is seen that for one actuator similar reductions are obtained from the geometric optimization as with those from the application of AVC. However, these are less than those achieved by solely geometric optimization, reported in reference [1]. The average AVC contribution using one actuator is of a similar value to the best reduction achieved using two actuators on the unoptimized structure geometry [2], and when using two actuators about 10 dB greater attenuation is achieved than when using three actuators on the unoptimized structure. Thus, the application of AVC is more effective per actuator for structures resulting from the combined optimization. Even though the geometric contributions are smaller than for the passive-then-active optimized structures, due to the larger AVC contributions the average overall attenuation achieved is similar when using one actuator. For two actuators, the values of attenuation resulting from the combined optimization are, on average, over 10 dB greater than for the passive-then-active optimization. Again, despite a comparatively smaller contribution from the geometry, the

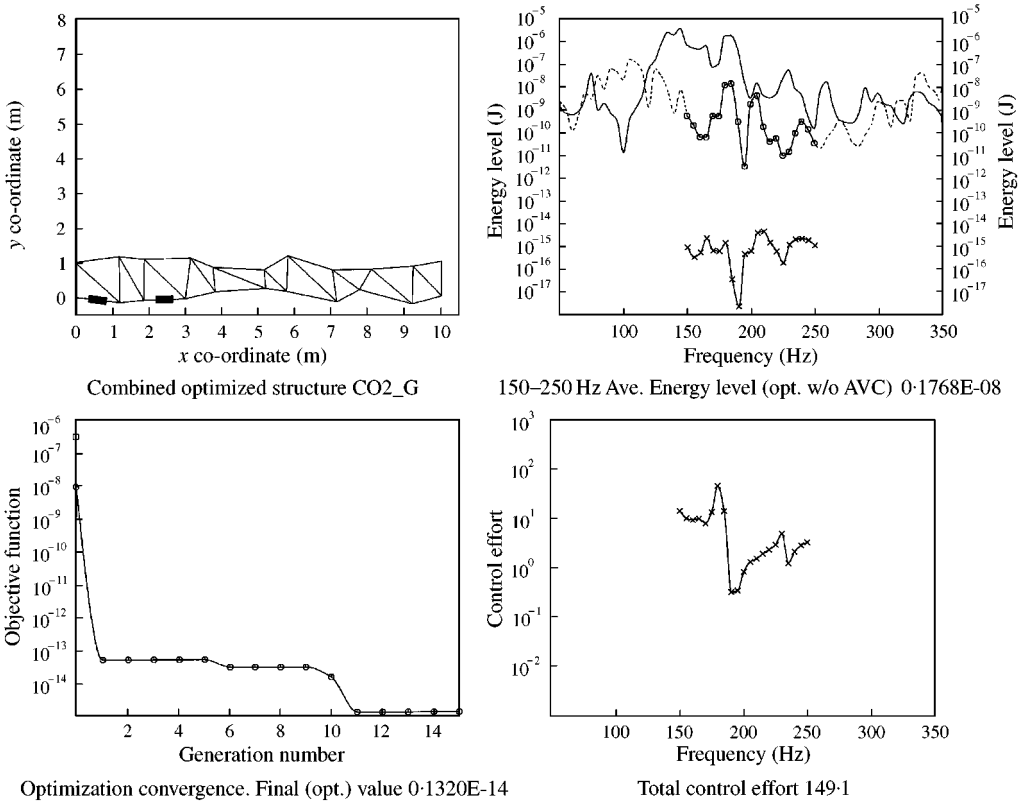

Figure 5. Best structure resulting from the combined optimization with two actuators, structure CO2_G. (Energy level: (—) unoptimized response; (– – –) optimized response; optimization window with AVC (—×—×—); and with AVC suppressed (—○—○—).)

success is due to large reductions attributed to AVC. It is noted that for an AVC system with a realistic noise floor, values of AVC attenuation at some frequencies would not be realized in practice, as discussed above. The values of frequency-averaged control effort are also given in Tables 3 and 4. A smaller variation between structures is seen than for the passive-then-active structures, of about 30 times for both one and two actuators. On a per actuator basis, compared with the passive-then-active structures, the average control effort is less for one actuator, but 3 times greater for two actuators. Again, these are much less than for an unoptimized structure. However, further comparison of the overall average attenuation and control effort for all strategies is discussed in section 5.

The effect of the significance of the actuator representation in the chromosome was briefly investigated. An extended chromosome was used, which comprised eight 16-bit indices, each of the range 0–1. These were combined to form a single index by summing and using a modulo one operator so that an index of 0–1 resulted. Again, the probabilities of each actuator combination occurring are equal if the indices are generated by uniformly distributed random processes, but the actuator representation is now about 18% of the chromosomes length. Studying the distribution of the actuator positions used at each evaluation in the optimization, it was apparent that more diversity was maintained throughout. However, this made little difference to the diversity of positions in the best structure in each generation. The final optimized structures had different geometries and actuator positions, but on average, yielded slightly less attenuation and required a higher

TABLE 3

Results summary for single-actuator combined optimized structures using the standard chromosome, ranked in order of performance

Rank	Structure	Geometric attenuation (dB)	AVC attenuation (dB)	Overall nominal attenuation (dB)	95% Probability limit attenuation (dB)	Control effort (N^2)	95% Probability limit control effort (N^2)
1	CO1 _ I	23·0	28·0	51·0	44·2	306	572
2	CO1 _ E	25·3	25·3	50·6	48·1	144	340
3	CO1 _ C	28·4	22·2	50·6	47·3	9·18	15·0
4	CO1 _ B	20·4	29·0	49·4	47·0	34·4	39·7
5	CO1 _ A	19·7	29·6	49·3	45·0	152	378
6	CO1 _ J	25·4	23·1	48·5	41·0	56·7	77·4
7	CO1 _ D	19·6	28·5	48·1	45·0	26·0	70·6
8	CO1 _ H	17·7	29·9	47·6	45·8	54·3	65·8
9	CO1 _ F	27·0	20·6	47·6	44·8	65·8	83·1
10	CO1 _ G	17·5	28·9	46·4	43·3	50·6	58·2
Average		21·0	27·5	48·7†	44·7	89·9	170

TABLE 4

Results summary for two-actuator combined optimized structures using the standard chromosome, ranked in order of performance

Rank	Structure	Geometric attenuation (dB)	AVC attenuation (dB)	Overall nominal attenuation (dB)	95% Probability limit attenuation (dB)	Control effort (N^2)	95% Probability limit control effort (N^2)
1	CO2 _ G	22·8	61·2	84·0	80·5	149	210
2	CO2 _ D	19·8	62·4	82·2	73·2	286	380
3	CO2 _ E	17·8	60·2	78·0	75·4	271	333
4	CO2 _ B	12·4	64·9	77·3	73·8	460	590
5	CO2 _ H	19·0	57·6	76·6	72·4	57·4	91·0
6	CO2 _ A	15·3	60·0	75·3	71·9	1310	2050
7	CO2 _ I	15·6	58·1	73·7	67·8	255	454
8	CO2 _ C	16·0	57·6	73·6	68·5	1770	3320
9	CO2 _ J	17·0	56·5	73·5	71·6	1410	1860
10	CO2 _ F	19·9	52·3	72·2	68·6	133	184
Average		16·7	60·3	78·4†	71·2	610	947

†As a consequence of the logarithmic scaling, the addition of the two average components of the nominal total attenuation does not result in the average total attenuation, as with the individual cases.

control effort. This allows the tentative suggestion that more successful optimization results when the geometry has more freedom to adapt around actuator positions. Further details are given in reference [12], where it is also noted that even using a chromosome representation biased towards mid-structural actuator positions, similar success can still be attained, even though the positions favoured from an unbiased representation occur at the structure base.

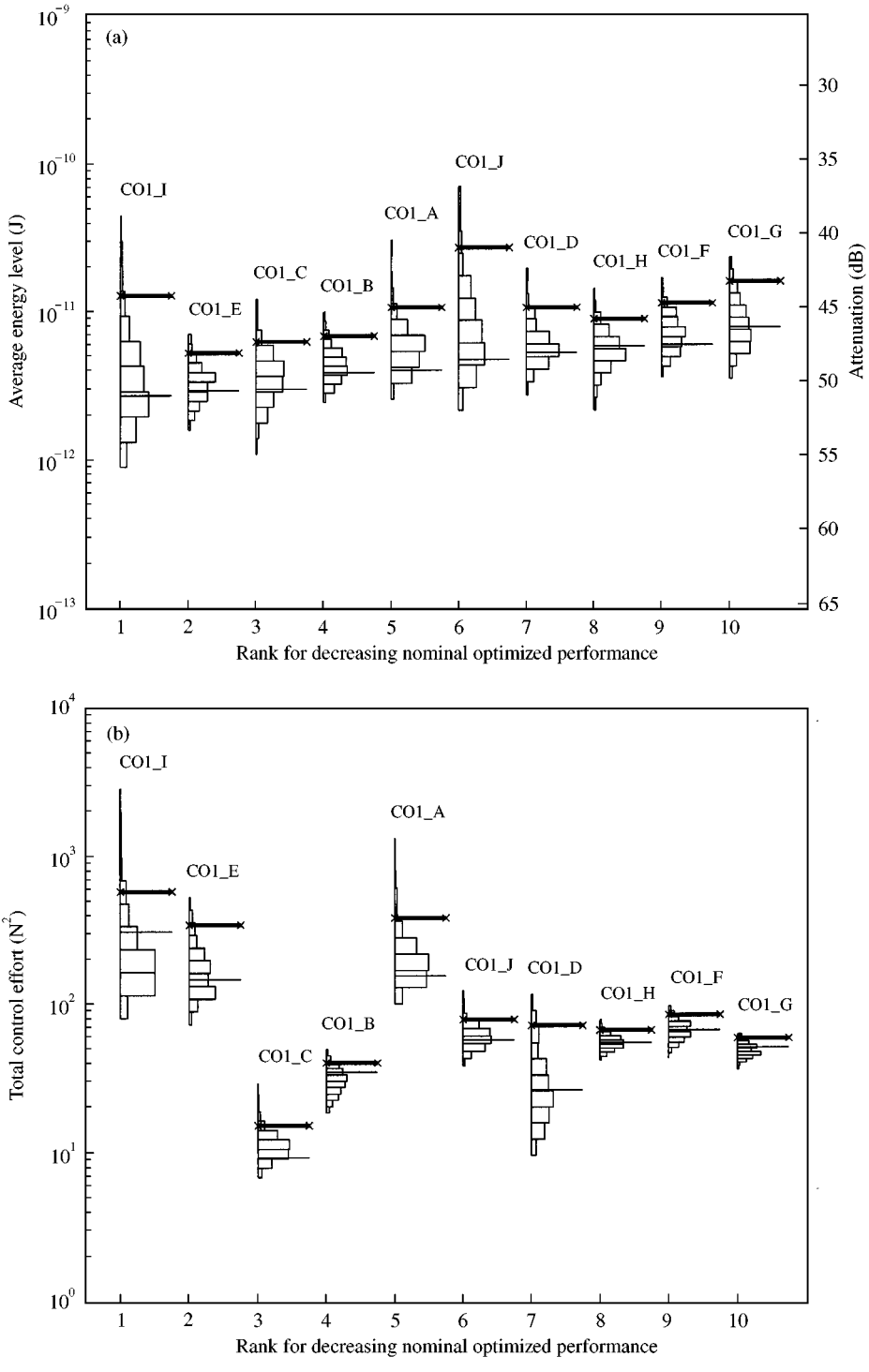

Figure 6. The statistical distribution and 95% probability limits (bold lines) for (a) the overall performance, and (b) the total control effort, for the structures resulting from the combined optimization using one actuator. Nominal values are shown by the thin lines.

4. ROBUSTNESS ANALYSIS

The optimized structures reported above are optimized for performance defined by a particular geometry, which itself is defined by a set of exact joint co-ordinates (corresponding to a joint position precision of 10 μm). So, if the joint positions were altered slightly, by manufacturing tolerances for example, the performance of the structure may vary significantly. In Parts I and II (the companion papers), through the robustness analyses performed, it has been seen that structures that often appeared to be the best design solutions on grounds of nominal performance, can often be very sensitive to small geometric structural perturbations. In practice, more *robust* structures are preferable.

The robustness analysis used here was the same as that used in references [1, 2], where more details were given. In brief, 300 sets of randomly generated uniformly distributed joint co-ordinate perturbations (of maximum size $\pm$ 10 mm) were applied to the structure and the performance and control effort re-evaluated for each set. A 95% probability limit is calculated that predicts the minimum vibration reduction that is expected for 95% of applied perturbations. For the AVC control effort, this limit allows a comparative representation of the expected electrical supply to the AVC system that would be required in practice. This size of the perturbations used was shown to be in a region representative of "small" perturbations [1].

Figure 6 shows the results of the perturbation analysis for the 10 combined optimized structures using one actuator. The histograms are ranked in order using the nominal optimized values. The histogram itself represents the distribution of the values of the energy level resulting from each perturbed geometry, and the bold horizontal line represents the 95% probability limit. Thus, it is seen that on the grounds of nominal performance structure CO1_I is the best single-actuator structure, although in practice structure CO1_E is likely to have a better performance as it has the lowest 95% probability limit. The control effort is also an important consideration when choosing a structure using an AVC system [2]. Structures CO1_I and CO1_E have similar levels of nominal control effort, and the 95% probability limit is about 2 times greater for each. The decision about which structure is chosen in practice is likely to be made by considering both the vibration reduction and the control effort required. In this case it is suggested that structure CO1_C would be the best choice, having slightly smaller expected vibration reduction than structure CO1_E, but the control effort required in practice is over 20 times less. Control effort is often perceived in linear terms, and thus this reduction is significant. The 95% probability limits for all the optimized structures reported above are given in Tables 1–4. Both the performance, which is expressed in decibels with respect to the unperturbed unoptimized structure without AVC, and the control effort are given. Averages values over the 10 structures in each case are also given. The combined optimization is seen to be more successful whether judged on grounds of nominal or perturbed performance. A comparison of the average perturbed performance of the structure resulting from all the optimization strategies is presented in the following section.

5. COMPARISON OF ALL OPTIMIZATION STRATEGIES

In the three parts of this set of companion papers, four different optimization strategies have been applied to the same structural vibration reduction problem. These were: geometric (*passive*) optimization; the application of AVC with optimally placed actuators to the original structure geometry (*active optimization*); and as reported above, passive-then-active and combined optimization strategies using both geometric

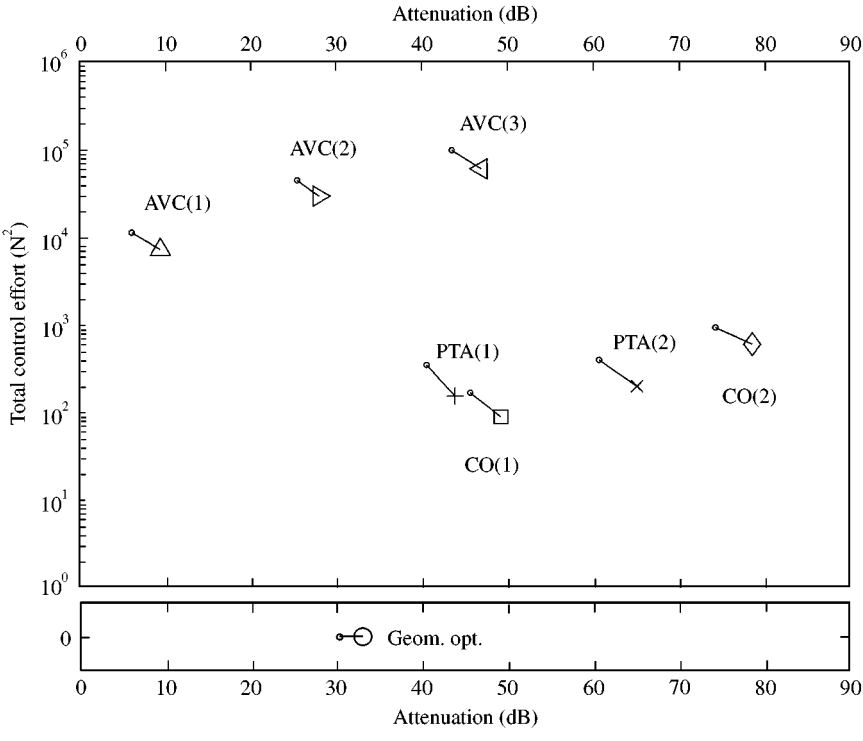

Figure 7. Comparison of nominal and perturbed optimized overall performance and total control effort for all optimized structures considered. Nominal performance key: solely geometric optimization (○); application of AVC on unoptimized structure (△, ▷, ◁) (1, 2, 3 actuators); passive-then-active optimization (+ , ×) (1, 2 actuators); combined optimization (□, ◇) (1,2 actuators). 95% probability limits are denoted by the end of the vectors emanating from the symbols.

optimization with an AVC system with optimally placed actuator positions. A brief comparison of the average performance obtained for each is now presented.

Figure 7 shows the average results for each strategy. The average energy level reduction (with respect to the unoptimized structure without AVC) for each strategy is plotted against the average control effort. The average attenuation geometric optimization is shown on a separate set of axes, as control effort is not applicable in this case.

Firstly, it is seen that the average vibration reduction achieved using optimization of the structure geometry only is equivalent to using an AVC system with two actuators on the unoptimized geometry. The structures resulting from the passive-then-active or the combined optimization strategy using one actuator provide an average overall vibration reduction that is similar to the application of AVC using three actuators on the unoptimized geometry. Thus, it is seen that the application of AVC to a structure produces greater overall reduction per actuator if the structure geometry undergoes optimization, either before or in combination with the geometric optimization. Also, the average control effort required by the structures resulting from the passive-then-active and combined optimization strategies is less than when using the unoptimized structure. Compared on either a per-actuator or per-attenuation basis, with geometric optimization the average control effort is about two orders of magnitudes less. Thus, the application of AVC is also more efficient when applied to a geometrically optimized structure.

The average 95% probability limits for the vibration reduction and the control effort are also shown in Figure 7 as vectors emanating from the larger symbols representing the

average values of nominal performance. The ends of the vectors represent the values of the 95% probability limits, so that, the westward extend of the vector indicates the average performance robustness and the northward extent indicates the average control effort robustness. Although the geometric optimization is seen to provide the most *performance robust* structures, there is little difference in this respect between these and the performance of the structures resulting from the other strategies. In terms of *control effort robustness* the structures resulting from the passive-then-active optimization with one actuator are seen to be the least robust, but again there is not much variation between these and the other structures. Thus, in general, no one optimization strategy produces structures which are more robust. However, as demonstrated in references [1, 2] and above in Figure 6, when making an individual choice of structure, consideration of the robustness for either the performance or control effort, where applicable, is important.

6. SUMMARY AND CONCLUSIONS

The optimization of a lightweight 2-D cantilever structure to reduce the average vibration transmission over a frequency band was performed. The first strategy (passive-then-active) applied AVC with optimally placed actuator positions on the structures with previously optimized geometries, using an exhaustive search for all the possible actuator positions. The second strategy (combined optimization) simultaneously optimized the structure geometry and the actuator positions, using genetic algorithms.

Good values of vibration reduction were achieved using both passive-then-active and the combined optimization strategies, using AVC with one and two actuators. The latter strategy produced the highest reductions. The combined optimization provided much larger reductions attributed to the AVC, despite smaller reductions due to the geometry. Thus, for the combined optimization the AVC is more effective per actuator. The structures required much less control effort than when using AVC on an unoptimized structure. Thus, the application of AVC is also more effective. The structures resulting from the passive-then-active optimization strategy would be more robust to the failure of the AVC system.

Robustness analyses were performed for all the structures, to find the expected performance and control effort required in the face of small geometric perturbations. It was seen that the best structure judged on grounds of nominal performance and control effort is not necessarily the best practical structure.

The average performance and control effort required of all the structures resulting from all the optimization strategies reported in this and the previous companion papers [1, 2] were presented together to allow comparison. From this it is clear that the application of AVC with optimized structure geometry produced better values of vibration reduction per actuator, and also required much less control effort. No optimization strategy was found to be significantly superior in terms of the robustness of either the performance or the control effort, although the importance of robustness when selecting the best practical structure was demonstrated in all the parts of the companion papers.

Finally, Table 5 shows the reduction in the average vibrational energy level and the control effort required for the geometric optimization, and for the three optimization methods incorporating AVC with two actuators. The control effort has been normalized by the *effective primary input control effort* (equal to $21\,N^2$ [2]). The relative inefficiency of using AVC on a geometrically unoptimized structure is readily apparent, as is the success of using the combined optimization strategy.

TABLE 5

Summary of average results of the four main optimization methods over the frequency band 150–250 Hz. The results for those methods using active vibration control are given for two actuators. Results for passive and active optimization types are taken from references [1, 2].

Optimization type	Optimization strategy	Overall reduction in average energy level of vibration (dB)	AVC control effort (normalized to primary control effort)
Passive	Optimized structure geometry.	33	0
Active	Apply AVC with optimal actuator positions on original geometry.	28	1400
Passive-then-active	Apply AVC with optimal actuator positions on previously geometrically optimized structures.	64	10
Combined	Simultaneous optimization of structure geometry and AVC actuator positions.	78	29

ACKNOWLEDGMENTS

The author acknowledges support in the form of a studentship from the Faculty of Engineering & Applied Science at the University of Southampton. He also wishes to thank Professors S. J. Elliott and A. J. Keane at the University of Southampton for their help with the work presented in this paper. All the computational work reported in this and the two previous companion papers were performed in the Computational Engineering and Design Centre at the University of Southampton.

REFERENCES

1. D. K. ANTHONY, S. J. ELLIOTT, and A. J. KEANE 2000 *Journal of Sound and Vibration* **229**, 505–528. Robustness of optimal design solutions to reduce vibration transmission in a lightweight 2-D structure. Part I: geometric redesign.
2. D. K. ANTHONY and S. J. ELLIOTT 2000 *Journal of Sound and Vibration* **229**, 529–548. Robustness of optimal design solutions to reduce vibration transmission in a lightweight 2-D structure. Part II: application of active vibration control techniques.
3. D. E. GOLDBERG 1989 *Genetic Algorithms in Search, Optimisation and Machine Learning*. Cambridge, MA: Addison-Wesley.
4. S. KIRKPATRICK, C. D. GELATT and M. P. VECCHI 1983 *Science* **220**, 671–680. Optimization by simulated annealing.
5. X. LIU, D. W. BEGG and D. R. MATRAVERS 1997 *Journal of Aerospace Engineering*. 119–125. Optimal topology/actuator placement design of structures using SA.
6. X. LIU, D. W. BEGG and R. J. FISHWICK 1998 *International Journal for Numerical Methods in Engineering* **41**, 815–830. Genetic approach to optimal topology/controller design of adaptive structures.
7. H. FURUYA 1995 *AIAA/ASME/ASCE/AHS Structures, Structural Dynamics & Materials Conference Collection of Technical Papers* Vol. 5, 3500–3505. Simultaneous design for configurations and actuator locations of space truss structures.

8. A. K. DHINGRA and B. H. LEE 1995 *International Journal for Numerical Methods in Engineering* **38**, 3383–3401. Multiobjective design of actively controlled structures using a hybrid optimization method.
9. G. CHEN, R. BRUNO and M. SALAMA 1991 *American Institute of Aeronautics and Astronautics Journal* **29**, 1327–1334. Optimal placement of active/passive members in truss structures using simulated annealing.
10. S. J. ELLIOTT and L. BILLET 1993 *Journal of Sound and Vibration* **163**, 295–310. Adaptive control of flexural waves propagating in a beam.
11. Dynamics Modelling Ltd., 1996. *The Options Design Exploration System*: *Reference Manual and User Guide—Version B1.1*. (for more information see: http://www.soton.ac.uk/ ~ ajk/options.ps).
12. D. K. ANTHONY 2000 *Ph.D. Thesis*, *University of Southampton*, *U.K.* Robust optimal design using passive and active methods of vibration control.